HHS Public Access

Author manuscript

Magn Reson Med. Author manuscript; available in PMC 2020 March 01.

Published in final edited form as:

Magn Reson Med. 2019 March ; 81(3): 1634–1644. doi:10.1002/mrm.27510.

Whole Knee Joint T_1 Values Measured *In Vivo* at 3T by Combined 3D Ultrashort Echo Time Cones Actual Flip Angle and Variable Flip Angle Methods

Ya-Jun Ma[1], **Wei Zhao**[1], **Lidi Wan**[1], **Tan Guo**[1], **Adam Searleman**[1], **Hyungseok Jang**[1], **Eric Y Chang**[2,1], and **Jiang Du**[1]

[1]Department of Radiology, University of California, San Diego, CA

[2]Radiology Service, VA San Diego Healthcare System, San Diego, CA

Abstract

Purpose: To measure T_1 relaxations for the major tissues in whole knee joints on a clinical 3T scanner.

Methods: The 3D UTE-Cones actual flip angle imaging (AFI) method was used to map the transmission radiofrequency field (B_1) in both short and long T_2 tissues, which was then used to correct the 3D UTE-Cones variable flip angle (VFA) fitting to generate accurate T_1 maps. Numerical simulation was carried out to investigate the accuracy of T_1 measurement for a range of T_2 values, excitation pulse durations, and B_1 errors. Then, the 3D UTE-Cones AFI-VFA method was applied to healthy volunteers (n=16) to quantify the T_1 of knee tissues including cartilage, meniscus, quadriceps tendon, patellar tendon, anterior cruciate ligament (ACL), posterior cruciate ligament (PCL), marrow and muscles at 3T.

Results: Numerical simulation showed that the 3D UTE-Cones AFI-VFA technique can provide accurate T_1 measurements (error less than 1%) when the tissue T_2 is longer than 1 ms and a 150 μs excitation RF pulse is used, and thus is suitable for most knee joint tissues. The proposed 3D UTE-Cones AFI-VFA method showed an average T_1 of 1098±67 ms for cartilage, 833±47 ms for meniscus, 800±66 ms for quadriceps tendon, 656±43 ms for patellar tendon, 873±38 ms for ACL, 832±49 ms for PCL, 379±18 ms for marrow and 1393±46 ms for muscles.

Conclusion: The 3D UTE-Cones AFI-VFA method allows volumetric T_1 measurement of the major tissues in whole knee joints on a clinical 3T scanner.

Keywords

ultrashort echo time; actual flip angle imaging; variable flip angle; knee joint

Corresponding Author: Jiang Du, Ph.D., jiangdu@ucsd.edu, University of California, San Diego, Department of Radiology, 200 West Arbor Drive, San Diego, CA 92103-8226, Phone (619) 471-0519, Fax (619) 471-0503.

INTRODUCTION

Human knee joints are composed of many soft tissues including articular cartilage, menisci, ligaments, tendons and muscles, all of which are important to the health of the joint (1–3). Accurate T_1 measurements of the major knee joint tissues can be used for optimization of signal intensity and image contrast (4). Additionally, T_1 relaxation is a fundamental property of a tissue and may be directly useful as a biomarker of disease or degeneration (5, 6), or used to measure other quantitative MRI biomarkers, such as the macromolecular proton fraction from magnetization transfer modeling or low frequency exchange information from $T_{1\rho}$ imaging (7–9).

Many T_1 measurement techniques have been proposed including inversion recovery (IR) and saturation recovery (SR) methods, as well as spoiled gradient recalled echo (SPGR)-based variable flip angle (VFA) and variable repetition time (VTR) methods (10–13). However, conventional MRI pulse sequences (such as SPGR and fast spin echo sequences) are of limited value for imaging deep radial and calcified cartilage, menisci, ligaments, bone and tendons because these tissues typically have T_2 values ranging from sub-milliseconds to several milliseconds and thus provide little or no detectable signal (14–16). In contrast, all of the major knee joint components, including both short and long T_2 tissues, can be imaged using ultrashort echo time (UTE) sequences with TEs less than 100 μs (6, 14–16). Thus, combining T_1 measurement techniques with UTE acquisitions has the potential for simultaneous T_1 mapping of the whole knee joint.

However, the IR based UTE (IR-UTE) method is inaccurate for T_1 measurement of short T_2 tissues because the required inversion pulse is too long (typically on the order of several milliseconds) on currently available clinical scanners to provide complete inversion of the short T_2 magnetization (17). The SR based UTE (SR-UTE) method provides more accurate T_1 measurements for short T_2 tissues (13) but would require long scan times for volumetric T_1 mapping. UTE-based VFA or VTR methods can provide volumetric T_1 mapping (17–22), but they suffer from high sensitivity to B_1 inhomogeneity (23–26). Obtaining an accurate B_1 map is crucial with VFA and VTR T_1 measurement approaches. Actual flip angle imaging (AFI) is a fast 3D B_1 mapping technique which has been successfully used for correction of VFA and VTR based T_1 measurements (23, 25).

UTE-AFI has been recently developed to map flip angles for both short and long T_2 tissues (22, 26). However, with conventional peak power limitations on the radiofrequency (RF) amplifiers of clinical scanners, the RF pulse duration must be increased in order to produce the large flip angle excitation (>40°) required for AFI. This longer RF pulse has reduced excitation efficiency (i.e. T_2 relaxation during the RF pulse) for short T_2 tissues, resulting in noticeable errors in the derived B_1 map when the tissue T_2 value is less than 0.5 ms (22). T_2 relaxation during the RF pulse results in smaller actual flip angles for short/ultrashort T_2 components than the nominal flip angle.

Previously, we have proposed using a UTE AFI-VTR method for accurate T_1 mapping of both short and long T_2 tissues of the knee (22). The effects of variable excitation efficiency were overcome by using an identical excitation pulse for the UTE-AFI and UTE-VTR

sequences (22). However, UTE AFI-VTR would require a long scan time for 3D high resolution knee imaging, making it unacceptable for clinical use (22). Since all major knee tissues other than bone have a T_2 value longer than 1 ms (11, 27–33), the B_1 map generated by the UTE-AFI method can still be used for B_1 correction of the faster VFA-based T_1 measurement for these tissues. Therefore, the UTE AFI-VFA method would be expected to provide accurate T_1 measurements of the soft tissues of the whole knee joint with much less scan time than the UTE AFI-VTR method.

In this study, numerical simulations were carried out to investigate the T_1 measurement accuracy of the UTE AFI-VFA method for the knee joint tissues with a variety of T_2 values on a clinical scanner. Then we applied the 3D UTE-Cones AFI-VFA method for *in vivo* whole knee imaging to measure T_1 values of cartilage, meniscus, quadriceps tendon, patellar tendon, anterior cruciate ligament (ACL), posterior cruciate ligament (PCL), marrow and muscles at 3T.

THEORY

Features of the 3D UTE-Cones pulse sequence with a single TR (Fig. 1a) have been described before (33–35). A series of 3D UTE-Cones acquisitions with variable flip angles are used for T_1 measurement. UTE-AFI can be achieved with the 3D dual TR UTE-Cones sequence (Fig. 1b) (22). Both the UTE-Cones AFI and the UTE-Cones VFA sequences use a short rectangular pulse (e.g. RF duration τ = 150 μs) for non-selective signal excitation (Fig. 1c), followed by spiral trajectory data acquisition with conical view ordering (Fig. 1d).

The generalized signal expressions of S_1 and S_2 for TR_1 and TR_2 of the AFI sequence (Fig. 1b) for both short and long T_2 tissues are expressed as follows (22):

$$S_1 = M_0 f_{xy}(\alpha, \tau, T_2) \frac{1 - E_2 + (1 - E_1) E_2 f_Z(\alpha, \tau, T_2)}{1 - E_1 E_2 f_Z^2(\alpha, \tau, T_2)} \quad [1]$$

$$S_2 = M_0 f_{xy}(\alpha, \tau, T_2) \frac{1 - E_1 + (1 - E_2) E_1 f_Z(\alpha, \tau, T_2)}{1 - E_1 E_2 f_Z^2(\alpha, \tau, T_2)} \quad [2]$$

with

$$E_1 = \exp\left(-TR_1/T_1\right),$$

$$E_2 = \exp\left(-TR_2/T_1\right).$$

M_0 is the equilibrium magnetization. $f_{xy}(\alpha, \tau, T_2)$ and $f_Z(\alpha, \tau, T_2)$ are the respective transverse and longitudinal magnetization mapping functions, which are described as follows (22, 37):

$$f_{xy}(\alpha, \tau, T_2) = e^{-\frac{\tau}{2T_2}} \alpha \text{sinc}\left(\sqrt{\alpha^2 - \left(\frac{\tau}{2T_2}\right)2}\right) \quad [3]$$

$$f_z(\alpha, \tau, T_2) = e^{-\frac{\tau}{2T_2}} \left(cos\left(\sqrt{\alpha^2 - (\frac{\tau}{2T_2})^2}\right) + \frac{\tau}{2T_2}\text{sinc}\left(\sqrt{\alpha^2 - (\frac{\tau}{2T_2})^2}\right)\right) \quad [4]$$

α is the nominal flip angle and τ is the duration of the rectangular excitation pulse.

With TR_1 and TR_2 that are short relative to T_1, the signal ratio r of S_1 and S_2 can be simplified using a first-order approximation for the exponential terms such that (23):

$$r = S_2/S_1 \approx \frac{1 + nf_Z(\alpha, \tau, T_2)}{n + f_Z(\alpha, \tau, T_2)} \quad [5]$$

where $n = TR_2/TR_1$. The ratio r can then be used as a T_1-independent measure of $f_Z(\alpha, \tau, T_2)$:

$$f_z(\alpha, \tau, T_2) \approx \frac{rn - 1}{n - r}. \quad [6]$$

For a tissue with $T_2 >> \tau$, $f_{xy}(\alpha, \tau, T_2)$ and $f_Z(\alpha, \tau, T_2)$ simplify to sin(α) and cos(α), respectively.

Thus, the actual flip angle α can be accurately estimated with the following equation (22, 23):

$$\alpha \approx arccos\left(\frac{rn - 1}{n - r}\right). \quad [7]$$

Then, the B_1 scaling factor (B_{1s}) is obtained by dividing the measured α by the nominal flip angle α_{nom}:

$$B_{1s} = \alpha/\alpha_{nom}. \quad [8]$$

B_{1s} is used to quantify the RF inhomogeneity, with $B_{1s} = 1$ corresponding to an unaltered RF field.

The signal equation of VFA based T_1 measurement with B_1 correction is expressed as follows (37):

$$S_{spgr} = M_0 sin(B_{1s}\theta)\frac{1-E_s}{1-E_s\cos(B_{1s}\theta)} \quad [9]$$

with $E_s = exp(-TR_s/T_1)$.

θ is the nominal flip angle and TR_s is the repetition time of the UTE-Cones sequence.

For tissues with T_2 values comparable to the RF duration τ, the excitation efficiency of the RF pulse decreases with T_2. The high dependency on tissue T_2 in $f_Z(\alpha, \tau, T_2)$ means that Eq. [7] is no longer accurate for the calculation of α, resulting in inaccurate B_{1s} estimates (22). This can result in estimation errors for VFA-based T_1 measurements because the method is sensitive to B_1 errors.

To investigate the accuracy of VFA T_1 measurement with AFI B_1 correction (UTE AFI-VFA) for tissues with a variety of T_2 values on a clinical scanner, numerical simulations were carried out as described below.

METHODS

The 3D UTE-Cones and 3D UTE-Cones AFI sequences (see Figure 1) were implemented on a 3T MR750 scanner (GE Healthcare Technologies, Milwaukee, WI). An 8-channel transmit/receive knee coil was used for both RF transmission and signal reception. Unique k-space trajectories were used in the UTE-Cones sequences that sampled data along evenly spaced twisted paths in the form of multiple cones (29–31). Data sampling began from the center of k-space and continued outwards. It began as soon as practical after the RF excitation with a minimal nominal delay time of 32 μs. Both RF and gradient spoiling were used to crush the remaining transverse magnetizations. In VFA UTE-Cones, the area of the gradient crushers was 180 mT·ms/m and the RF phase increment was 169°. In UTE-Cones AFI, the areas of gradient crushers in TR_1 and TR_2 were 180 and 900 mT·ms/m respectively, and the RF phase increment was 39° (22). The UTE-Cones sequence allowed anisotropic resolution (e.g., higher in-plane resolution and thicker slices) to provide an improved signal to noise ratio (SNR) and a reduced scan time relative to isotropic imaging (30, 31).

Simulation

Numerical simulation was performed to investigate the accuracy of the proposed UTE AFI-VFA T_1 measurement for relatively short T_2 tissues. The UTE AFI-VFA technique is expected to accurately measure T_1 for long T_2 tissues. Simulated rectangular RF pulses used for signal excitation in both the 3D UTE AFI and VFA sequences had identical durations and ranged from 0.1 to 300 μs. T_2 values of simulated tissues ranged from 0 to 5 ms. The B_1 scaling factors and the ratio between f_{xy} and sin $(B_{1s}\theta)$ measured with different nominal flip angles (range from 0° to 90°) for short T_2s were also investigated with a pulse duration of

150 μs. This ratio was calculated to investigate whether the obtained B_{1s} could correct the transverse part of the excitation. The T_1 measurement accuracy with the VFA method depends on the accurate correction of both transverse and longitudinal magnetizations after excitation. The T_1 value was set to a constant of 800 ms and M_0 was set to 1. The sequence parameters for UTE AFI and VFA sequences were adjusted as follows: 1) UTE-AFI: TR_1/TR_2 = 20/100 ms and flip angle = 45°; 2) UTE-VFA: TR = 20 ms, and flip angle = 5°, 10°, 20° and 30°. B_1 scaling factors and T_1 values with and without B_1 correction were calculated for three nominal B_1 scaling factors (B_{1n}): 0.8, 1 and 1.2.

In Vivo* Study—In vivo* whole knee imaging was carried out on 16 healthy volunteers (aged 20–49 years, mean age 34 years; 7 males, 9 females). Informed consent was obtained from all subjects in accordance with guidelines of the institutional review board. The 3D UTE-Cones AFI and VFA sequences were used to scan these knee joints using the same field of view (FOV) of 15×15×10.8 cm^3 and receiver bandwidth of 166 kHz. Other sequence parameters were: 1) 3D UTE-Cones AFI: TR_1/TR_2 = 20/100 ms, flip angle = 45°, acquisition matrices of 128×128×18, readout duration = 924 μs and a total scan time of 4 min 57 sec; 2) 3D VFA UTE-Cones: TR = 20 ms , flip angle = 5°, 10°, 20° and 30°, acquisition matrices of 256×256×36, undersampling factor of 0.9, readout duration = 1644 μs and a total scan time of 9 min 28 sec.

Data Analysis

Before T_1 calculation, motion registration was performed for all datasets using the Elastix open source software (38). Rigid registration was carried out first to correct for tissue translations and rotations, and then non-rigid registration was applied for further fine adjustment (such as scaling and shearing), which is particularly important for soft tissues. The Levenberg-Marquardt algorithm was used to solve the non-linear fitting of Eq. [9] for VFA T_1 measurement. The analysis algorithms written in Matlab (The Mathworks, Inc., Natick, MA) were applied to the DICOM images obtained from the 3D UTE-Cones AFI and VFA UTE-Cones protocols described above. Both T_1 values and fitting errors were calculated. Manually drawn regions-of-interest for the 16 *in vivo* knees were used to measure the mean and standard deviation T_1 values of various tissues including the articular cartilage, meniscus, quadriceps tendon, patellar tendon, ACL, PCL, marrow and muscles.

RESULTS

The simulation results with variable pulse durations for a range of T_2s are shown in Figure 2. The top two rows show the theoretical longitudinal (M_z or $f_z(\alpha, \tau, T_2)$) and transverse (M_{xy} or $f_{xy}(\alpha, \tau, T_2)$) magnetizations calculated by Eqs. [3] and [4]. Longer RF pulses were shown to be less effective than shorter ones in generating M_{xy} for shorter T_2 tissues. M_z and M_{xy} approached $cos(\alpha)$ and $sin(\alpha)$, respectively, as T_2 increased. The third row in Figure 2 shows the estimated B_1 scaling factors B_{1s} computed using the AFI method with Eqs. [7] and [8]. As expected, the measured B_{1s} were more accurate when using shorter RF pulses and when imaging longer T_2 species. Otherwise, the estimated B_{1s} were smaller than the nominal values.

The bottom two rows show the simulation results of T_1 measurements using the VFA method without and with B_1 correction. The B_1-uncorrected T_1 values show significant estimation errors and increased with larger values of the nominal B_1 scaling factor B_{1n}. Overall, the T_1 values generated by the B_1-corrected VFA method were much more accurate than the T_1 values measured by the B_1-uncorrected VFA method. However, T_1 estimation errors still existed in the B_1-corrected T_1 values when T_2 values were shorter than 0.5 ms, and the errors became larger with increased B_{1n}. All three of the B_1-corrected T_1 maps were separated into two regions by dashed black lines: the T_1 estimation errors were higher than 1% in the bottom left portions (triangular shaped area) and the T_1 estimation errors in the other portions were lower than 1%. Thus, we found that when an excitation pulse with a duration of 150 μs is used for imaging tissues with T_2 values greater than 1 ms, the B_1-corrected T_1 value measured by the AFI-VFA method is accurate with less than 1% estimation error in the setting of up to 20% B_1 inhomogeneity.

The simulation curves with a range of nominal flip angles for the four short T_2s (i.e. 0.2 ms, 0.3 ms, 0.5 ms and 1 ms) are shown in Figure 3. Both B_1 scaling factors and the ratio between f_{xy} and $\sin\left(B_{1s}\theta\right)$ slightly changed with different nominal flip angles. More changes can be found when tissue T_2 is shorter. So for shorter T_2s, a single correction factor is not good enough to correct the excitation errors in different flip angles for VFA T_1 measurement as shown in the last row of Figure 2. However, both B_{1s} and the ratio almost stay constant for flip angles lower than 50° when T_2 is 1 ms or longer, which demonstrate the accuracy of the proposed AFI-VFA T_1 measurement method for tissues with T_{2s} longer than 1 ms.

Since the articular cartilage, meniscus, quadriceps tendon, patellar tendon, ACL, PCL, marrow and muscles all have T_2 values longer than 1 ms, the B_1-corrected VFA method with a 150 μs long excitation pulse should be suitable for the measurement of T_1 values of these tissues. The signal intensities of the tissues have been measured before and after registration. There were almost no signal intensity changes due to the motion registration. Figure 4 shows T_1 fitting results for various knee joint tissues of a representative healthy volunteer (age 35, male). All the data show excellent fittings. The proposed 3D UTE-Cones AFI-VFA method showed a T_1 value of 832±18 ms for meniscus, 779±7 ms for quadriceps tendon, 637±16 ms for patellar tendon, 870±13 ms for ACL, 819±17 ms for PCL, 1133±40 ms for cartilage, 386±2 ms for marrow and 1406±63 ms for muscles of this volunteer.

Figure 5 shows T_1 mapping results of the knee of the same healthy volunteer as above. T_1 maps generated by the proposed 3D UTE-Cones AFI-VFA method are shown in Figs. 5d to 5f. For comparison, the T_1 maps generated by the 3D UTE-Cones VFA method without B_1 correction are shown in Figs. 5g to 5i. T_1 estimation errors induced by B_1 inhomogeneity, which are more severe in regions close to the coil boundary, have been corrected by the proposed 3D UTE-Cones AFI-VFA method. Corresponding B_{1s} maps are shown in Figs. 5j to 5l. As expected, lower B_{1s} values can be found in cortical bone regions due to lower excitation efficiency.

Table 1 summarizes T_1 measurements by the proposed 3D UTE-Cones AFI-VFA method for the principal knee joint tissues of healthy volunteers (n = 16). The proposed 3D UTE-Cones AFI-VFA method showed a mean T_1 value and standard deviation of 833 ± 47 ms for

meniscus, 800 ± 66 ms for quadriceps tendon, 656 ± 43 ms for patellar tendon, 873 ± 38 ms for ACL, 832 ± 49 ms for PCL, 1098 ± 67 ms for cartilage, 379 ± 18 ms for marrow and 1393 ± 46 ms for muscles.

DICUSSION

We have demonstrated that the proposed 3D UTE-Cones AFI-VFA method can accurately measure T_1 values for most major tissues of the whole knee joint. Simulation shows that the proposed 3D UTE-Cones AFI-VFA method provides accurate T_1 measurements for tissues with T_2 values longer than 1 ms. Since most knee tissues have T_2s longer than 1 ms (meniscus: 5–8 ms, ligament and tendon: 4–10 ms, cartilage: 27–43 ms, muscle: 32–50 ms and fat: ~133 ms) (11, 27–33), accurate T_1 maps were obtained using the proposed method to provide *in vivo* knee measurements in 16 healthy volunteers.

Due to the high sensitivity in VFA T_1 measurements to B_1 errors, obtaining an accurate B_1 map is crucial. AFI is a fast 3D B_1 mapping technique which fits very well with VFA based T_1 corrections. It has been used for volumetric B_1 mapping of brain, body, and musculoskeletal tissues (23, 40, 41). UTE-AFI techniques using radial trajectories have been implemented for B_1 mapping of short T_2 tissues on both clinical 3T and 9.4T MRI systems (20, 26). Most recently, we have implemented the 3D UTE-Cones based AFI sequence on a clinical 3T scanner (22). 3D UTE-Cones employs a spiral trajectory data acquisition with conical view ordering, which provide the flexibility to stretch each spiral interleave to vastly reduce the total number of interleaves. Thus, combined with the ability for anisotropic resolution, the 3D UTE-Cones data acquisition is much more efficient than the radial UTE acquisition (33, 34).

As shown in the simulation study and a previous cortical bone study (22), the VFA T_1 maps did not show much improvement after B_1 correction for very short T_2 tissues such as cortical bone. However, for tissues with T_2 values longer than 1 ms (much longer than pulse duration of 150 μs), the obtained B_{1s} is almost accurate and AFI-VFA can provide accurate T_1 measurement. The coverage of the simulated nominal B_1 scaling factors B_{1n} from 0.8 to 1.2 should be wide enough for most cases of *in vivo* knee imaging. Thus, the proposed 3D UTE-Cones AFI-VFA method was able to accurately measure T_1 of all the major knee tissues except for bone.

To our best knowledge, this study is the first to report the T_1 values for all the soft tissues in the human knee joint *in vivo*. Most of previous T_1 measurement studies focused on the articular cartilage, meniscus and muscle. The T_1 values of the ligaments including quadriceps tendon, patellar tendon, ACL and PCL have been barely studied since they are not detected by clinical sequences due to their relatively short T_2 values. Our measured T_1 values for cartilage (~1098 ms), muscle (~1393 ms) and marrow (~379 ms) at 3T are comparable with previous 3T studies. For example, Stanisz et. al. reported T_1 values of 1156 ms for cartilage and 1412 ms for skeletal muscle (11); Gold et. al. reported T_1 values of 1240 ms for cartilage, 1420 ms for skeletal muscle and 365 ms for marrow (33); and Jordan et. al. reported T_1 values of 1016 ms for cartilage, 1256 ms for muscle and 381 ms for

marrow (42). We recently measured *in vivo* cortical bone T_1 values of around 220 ms using a related 3D UTE-Cones AFI-VTR method (22).

Magnetization transfer (MT) effects were not considered for both the AFI B_1 scaling factor and VFA T_1 quantification in this study. Since most tissues in our study such as cartilage and menisci have high macromolecular contents, MT effects can lead to T_1 measurement errors for the AFI-VFA method (43–45). Further work should consider and correct MT effects for more accurate T_1 measurement. In addition, an interesting finding is that the B_{1s} maps in Figure 5 show contrast between fat and other tissues. This may be a result from the MT effect since fat has negligible MT effect in comparison to other tissues. Another possible explanation for the contrast is the different dielectric properties of fat and other tissues (46). Secondary B_1 field components can be generated by tissue-specific induced current densities. Thus, the higher B_{1s} values observed in cartilage, menisci, and muscle may also result from greater induced current densities, since their conductivity and permittivity values are much greater than those of fat (47). Previous authors have investigated tissue dielectric properties based on the transmit B_1 maps (48, 49).

There are also several limitations of this study. First, the total data acquisition time is relatively long, in part due to the parameters selected for high accuracy, high image resolution and broad spatial coverage. A number of strategies can be employed to reduce the total scan time, including decreasing the total number of FAs for VFA (10), using lower resolution for B_1 mapping and advanced techniques for image reconstruction such as parallel imaging and compressed sensing reconstruction (50). Second, fat and chemical shift artifacts (which produce ring artifacts in 3D UTE-Cones imaging) may lead to errors in T_1 estimation, necessitating some form of fat-water signal separation to improve accuracy (51).

CONCLUSION

The 3D UTE-Cones AFI-VFA method provides a robust technique for volumetric T_1 mapping of all the soft tissues in knee joints *in vivo* with a clinical 3T scanner, including the articular cartilage, meniscus, quadriceps tendon, patellar tendon, ACL, PCL, marrow and muscles.

ACKNOWLEDGEMENTS

The authors acknowledge grant support from NIH (1R01 AR062581, 1R01 AR068987, and T32EB005970), the Veterans Affairs (1I01CX001388 and I01RX002604), and GE Healthcare.

REFERENCES

1. Brandt KD, Radin EL, Dieppe PA, Putte L. Yet more evidence that osteoarthritis is not a cartilage disease (Editorial). Ann Rheum Dis 2006;65:1261–1264. [PubMed: 16973787]
2. Hunter DJ, Zhang YQ, Niu JB, Tu X, Amin S, Clancy M, Guermazi A, Grigorian M, Gale D, Felson DT. The association of meniscal pathologic changes with cartilage loss in symptomatic knee osteoarthritis. Arthritis Rheum 2006;54:795–801. [PubMed: 16508930]
3. Tan AL, Toumi H, Benjamin M, Grainger AJ, Tanner SF, Emery P, McGonagle D. Combined high-resolution magnetic resonance imaging and histological examination to explore the role of ligaments and tendons in the phenotypic expression of early hand osteoarthritis. Ann Rheum Dis 2006;65:1267–1272. [PubMed: 16627540]

4. Zawadzki MB, Gillan GD, Nitz WR. MP-RAGE: a three-dimensional, T1-weighted, gradient-echo sequence—initial experience in the brain. Radiology 1992;182(3):769–775. [PubMed: 1535892]
5. Burstein D, Velyvis J, Scott KT, Stock KW, Kim YJ, Jaramillo D, Gray ML. Protocol issues for delayed Gd (DTPA) 2-enhanced MRI (dGEMRIC) for clinical evaluation of articular cartilage. Magn Reson Med 2001;45(1):36–41. [PubMed: 11146483]
6. Tiderius CJ., Olsson LE, Leander P, Ekberg O, & Dahlberg L (2003). Delayed gadolinium-enhanced MRI of cartilage (dGEMRIC) in early knee osteoarthritis. Magn Reson Med 2003;49(3):488–492. [PubMed: 12594751]
7. Ma YJ, Chang EY, Carl M, Du J. Quantitative magnetization transfer ultrashort echo time imaging using a time-efficient 3D multispoke Cones sequence. Magn Reson Med 2017;10.1002/mrm.26716.
8. Ma YJ, Carl M, Shao H, Tadros AS, Chang EY, Du J. Three-dimensional ultrashort echo time cones T1ρ (3D UTE-cones-T1ρ) imaging. NMR Biomed 2017;10.1002/nbm.3709.
9. Ma YJ, Carl M, Searleman A, Lu X, Chang EY, Du J. 3D adiabatic T1ρ prepared ultrashort echo time cones sequence for whole knee imaging. Magn Reson Med 2018;10.1002/mrm.27131.
10. Deoni SC, Rutt BK, Peters TM. Rapid combined T_1 and T_2 mapping using gradient recalled acquisition in the steady state. Magn Reson Med 2003;49:515–26. [PubMed: 12594755]
11. Stanisz GJ, Odrobina EE, Pun J, Escaravage M, Graham SJ, Bronskill MJ, Henkelman RM. T_1, T_2 relaxation and magnetization transfer in tissue at 3T. Magn Reson Med 2005;54:507–12. [PubMed: 16086319]
12. Stikov N, Boudreau M, Levesque IR, Tardif CL, Barral JK, Pike GB. On the accuracy of T_1 mapping: searching for common ground. Magn Reson Med 2015;73:514–22. [PubMed: 24578189]
13. Techawiboonwong A, Song HK, Leonard MB, Wehrli FW. Cortial bone water: in vivo quantification with ultrashort echo-time MR imaging. Radiology 2008;248:824–833. [PubMed: 18632530]
14. Chang EY, Du J, Bae WC, Chung CB. Qualitative and Quantitative Ultrashort Echo Time Imaging of Musculoskeletal Tissues. Semin Musculoskelet Radiol 2015;19(4):375–386. [PubMed: 26583365]
15. Du J, Carl M, Diaz E, Takahashi A, Han E, Szeverenyi NM, Chung CB, Bydder GM. Ultrashort TE T1rho (UTE T1rho) imaging of the Achilles tendon and meniscus. Magn Reson Med 2010;64(3): 834–842. [PubMed: 20535810]
16. Du J, Carl M, Bae WC, Statum S, Chang EY, Bydder GM, Chung CB. Dual inversion recovery ultrashort echo time (DIR-UTE) imaging and quantification of the zone of calcified cartilage (ZCC). Osteoarthritis Cartilage 2013;21(1):77–85. [PubMed: 23025927]
17. Horch RA, Gochberg DF, Nyman JS, Does MD. Clinically compatible MRI strategies for discriminating bound and pore water in cortical bone. Magn Reson Med 2012;68(6):1774–1784. [PubMed: 22294340]
18. Chen J, Chang EY, Carl M, Ma Y, Shao H, Chen B, Wu Z, Du J. Measurement of bound and pore water T_1 relaxation times in cortical bone using three-dimensional ultrashort echo time cones sequences. Magn Reson Med 2017;77:2136–45. [PubMed: 27263994]
19. Du J, Bydder GM. Qualitative and quantitative ultrashort-TE MRI of cortical bone. NMR Biomed 2013;26:489–506. [PubMed: 23280581]
20. Han M, Larson PEZ, Krug R, Rieke V. Actual flip angle imaging to improve T_1 measurement for short T_2 tissues. In: Proceedings of the 23rd Annual Meeting of ISMRM, Toronto, Ontario, Canada 2015, p501.
21. Han M, Rieke V, Scott SJ, Ozhinsky E, Salgaonkar VA, Jones PD, Larson PE, Diederich CJ, Krug R. Quantifying temperature-dependent T1 changes in cortical bone using ultrashort echo-time MRI. Magn Reson Med 2015;74(6):1548–55. [PubMed: 26390357]
22. Ma YJ, Lu X, Carl M, et al. Accurate T1 mapping of short T2 tissues using a three-dimensional ultrashort echo time cones actual flip angle imaging variable repetition time (3D UTE-Cones AFI-VTR) method. Magn Reson Med 2018; 10.1002/mrm.27066.
23. Yarnykh VL. Actual flip-angle imaging in the pulsed steady state: a method for rapid three-dimensional mapping of the transmitted radiofrequency field. Magn Reson Med 2007;57:192–200. [PubMed: 17191242]

24. Deoni SC. High-resolution T_1 mapping of the brain at 3T with driven equilibrium single pulse observation of T_1 with high-speed incorporation of RF field inhomogeneities (DESPOT1-HIFI). J Magn Reson Imaging 2007;26:1106–1111. [PubMed: 17896356]
25. Yarnykh VL. Optimal radiofrequency and gradient spoiling for improved accuracy of T_1 and B_1 measurements using fast steadystate techniques. Magn Reson Med 2010;63:1610–1626. [PubMed: 20512865]
26. Kobayashi N, Garwood M. B_1 mapping of short T_2* spins using a 3D radial gradient echo sequence. Magn Reson Med 2014;71:1689–99. [PubMed: 23754634]
27. Robson MD, Gatehouse PD, Bydder M, Bydder GM. Magnetic resonance: an introduction to ultrashort TE (UTE) imaging. J Comput Assist Tomog 2003;27(6):825–46.
28. Wilson KJ, Surowiec RK, Ho CP, Devitt BM, Fripp J, Smith WS, LaPrade RF. Quantifiable imaging biomarkers for evaluation of the posterior cruciate ligament using 3-T magnetic resonance imaging: a feasibility study. Orthopaedic journal of sports medicine 2016; 4(4): 2325967116639044.
29. Liu F, Kijowski R. Assessment of different fitting methods for in-vivo bi-component T2* analysis of human patellar tendon in magnetic resonance imaging. Muscles, ligaments and tendons journal 2017; 7(1): 163–172.
30. Williams A, Qian Y, Golla S, Chu CR. UTE-T2∗ mapping detects sub-clinical meniscus injury after anterior cruciate ligament tear. Osteoarthritis and cartilage 2012;20(6):486–494. [PubMed: 22306000]
31. Du J, Diaz E, Carl M, Bae W, Chung CB, Bydder GM. Ultrashort echo time imaging with bicomponent analysis. Magn Reson Med 2012; 67(3): 645–649. [PubMed: 22034242]
32. Ma YJ, Chang EY, Bydder GM, Du J. Can ultrashort-TE (UTE) MRI sequences on a 3-T clinical scanner detect signal directly from collagen protons: freeze–dry and D2O exchange studies of cortical bone and Achilles tendon specimens. NMR in Biomed 2016; 29(7): 912–917.
33. Gold GE, Han E, Stainsby J, Wright GA, Brittain J, Beaulieu C. Musculoskeletal MRI at 3.0T: relaxation times and image contrast. Am J Neuroradiol 2004;183:343–350.
34. Gurney PT, Hargreaves BA, Nishimura DG. Design and analysis of a practical 3D cones trajectory. Magn Reson Med 2006;55:575–582. [PubMed: 16450366]
35. Carl M, Bydder GM, Du J. UTE imaging with simultaneous water and fat signal suppression using a time-efficient multispoke inversion recovery pulse sequence. Magn Reson Med 2016;76:577–582. [PubMed: 26309221]
36. Ma YJ, Zhu Y, Lu X, Carl M, Chang EY, Du J. Short T2 imaging using a 3D double adiabatic inversion recovery prepared ultrashort echo time cones (3D DIR-UTE-Cones) sequence. Magn Reson Med 2017;10.1002/mrm.26908.
37. Sussman MS, Pauly JM, Wright GA. Design of practical T2-selective RF excitation (TELEX) pulses. Magn Reson Med 1998;40:890–899. [PubMed: 9840834]
38. Hurley SA, Yarnykh VL, Johnson KM, Field AS, Alexander AL, Samsonov AA. Simultaneous variable flip angle–actual flip angle imaging method for improved accuracy and precision of three-dimensional T_1 and B_1 measurements. Magn Reson Med 2012;68:54–64. [PubMed: 22139819]
39. Klein S, Staring M, Murphy K, Viergever MA, Pluim JP. Elastix: a toolbox for intensity-based medical image registration. IEEE transactions on medical imaging 2010;29(1): 196–205. [PubMed: 19923044]
40. Sinclair CD, Samson RS, Thomas DL, Weiskopf N, Lutti A, Thornton JS, Golay X. Quantitative magnetization transfer in in vivo healthy human skeletal muscle at 3 T. Magn Reson Med 2010;64:1739–48. [PubMed: 20665899]
41. Baudrexel S, Nürnberger L, Rüb U, Seifried C, Klein JC, Deller T, Steinmetz H, Deichmann R, Hilker R. Quantitative mapping of T1 and T2* discloses nigral and brainstem pathology in early Parkinson's disease. Neuroimage 2010;51:512–20. [PubMed: 20211271]
42. Jordan CD, Saranathan M, Bangerter NK, Hargreaves BA, Gold GE. Musculoskeletal MRI at 3.0T and 7.0T: Relaxation Times and Image Contrast. ORS Annual Meeting 2012, n0461.
43. Mossahebi P, Yarnykh VL, Samsonov A. Analysis and correction of biases in cross-relaxation MRI due to biexponential longitudinal relaxation. Magn Reson Med 2014;71(2):830–8. [PubMed: 23440870]

44. Bieri O, Scheffler K. On the origin of apparent low tissue signals in balanced SSFP. Magn Reson Med 2006;56(5):1067–1074. [PubMed: 17036284]
45. Mossahebi P, Yarnykh VL, Samsonov A. Analysis and correction of biases in cross-relaxation MRI due to biexponential longitudinal relaxation. Magn Reson Med 2014;71(2):830–838. [PubMed: 23440870]
46. Brink WM, Börnert P, Nehrke K, Webb AG. Ventricular B1+ perturbation at 7 T–real effect or measurement artifact? NMR in Biomedicine 2014;27(6):617–20. [PubMed: 24733571]
47. Gabriel S, Lau RW, Gabriel C. The dielectric properties of biological tissues: III. Parametric models for the dielectric spectrum of tissues. Phys Med Biol 1996;41(11):2271. [PubMed: 8938026]
48. Voigt T, Katscher U, Doessel O. Quantitative conductivity and permittivity imaging of the human brain using electric properties tomography. Magn Reson Med 2011;66(2):456–66. [PubMed: 21773985]
49. Bulumulla SB, Lee SK, Yeo DT. Conductivity and permittivity imaging at 3.0 T. Concepts in Magn Reson Part B: Magn Reson Eng 2012;41(1):13–21.
50. Lustig M, Donoho D, Pauly JM. Sparse MRI: The application of compressed sensing for rapid MR imaging. Magn Reson Med 2007;58:1182–95. [PubMed: 17969013]
51. Rakow-Penner R, Daniel B, Yu H, Glover AS, Glover GH. Relaxation times of breast tissue at 1.5T and 3T measured using IDEAL. J Magn Reson Imaging 2006; 23:87–91. [PubMed: 16315211]

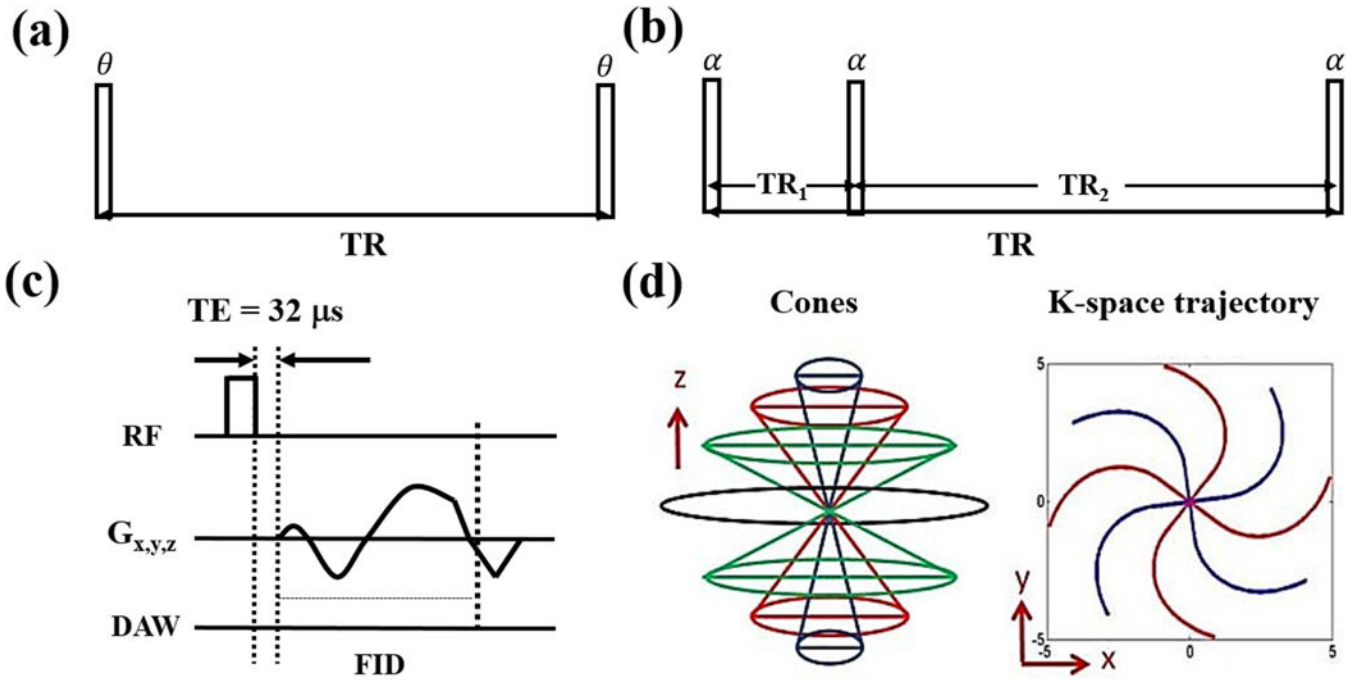

Figure 1.

The 3D UTE-Cones sequence with a single TR is used for T_1 measurement with the variable flip angle (VFA) method (a). The 3D UTE-Cones actual flip angle imaging (AFI) sequence employs a pair of interleaved TRs for accurate B_1 mapping (b), which together with the VFA method provides accurate T_1 measurements. In these two UTE-Cones sequences, a short rectangular pulse is used for signal excitation followed by 3D spiral sampling with a very short TE of 32 μs (c). The spiral trajectories are arranged with conical view ordering (d).

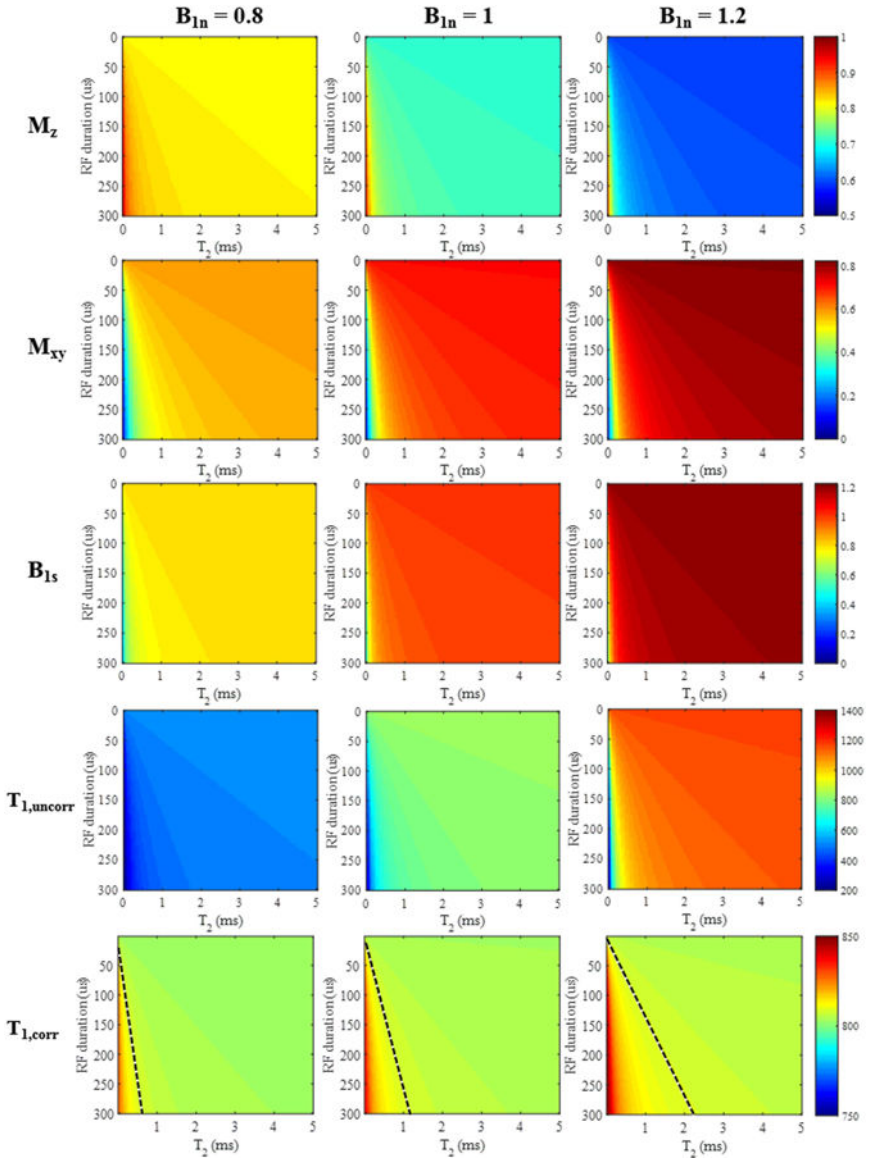

Figure 2.

Simulation results for different T_2 tissues (T_2 values from 0 to 5 ms) with rectangular RF pulse excitation (durations from 0.1 to 300 μs). The top two rows show color maps corresponding to the longitudinal (M_Z or $f_Z(\alpha, \tau, T_2)$) and transverse (M_{xy} or $f_{xy}(\alpha, \tau, T_2)$) magnetizations calculated from Eqs. [3] and [4]. The third row shows the resulting B_{1s} scaling factors obtained by the AFI method (i.e. Eqs. [7] and [8]). T_1 values (units of ms) generated by the VFA method are shown without (fourth row) and with B_{1s} correction (fifth row). For the B_1-corrected T_1 results, a dashed black line was drawn such that the region to the left of the line had a T_1 estimation error greater than 1% and the region to the right had an estimation error less than 1%. The columns represent simulation results with nominal B_1 scaling factors B_{1n} of 0.8, 1, and 1.2, respectively.

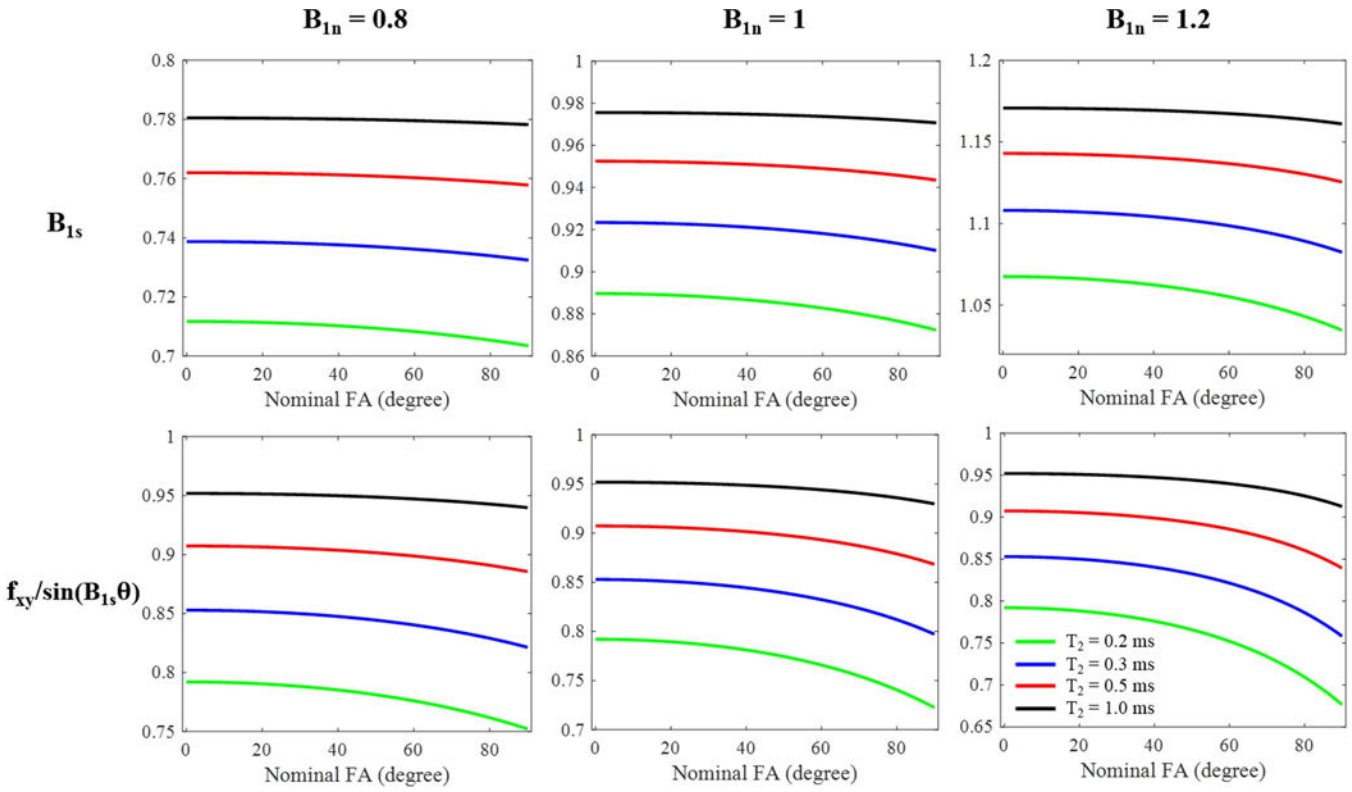

Figure 3.

Simulation curves for different T_2 tissues (green: 0.2 ms, blue: 0.3 ms, red: 0.5 ms and black: 1 ms) with rectangular RF pulse excitation (nominal FA from 0° to 90°; pulse duration τ = 150 μs). The first row shows the resulting B_1 scaling factors obtained by the AFI method (i.e. Eqs. [7] and [8]). The second row shows the ratio between f_{xy} in Eq. [3] and $\sin(B_{1s}\theta)$ in Eq. [9]. The columns represent simulation results with nominal B_1 scaling factors B_{1n} of 0.8, 1, and 1.2, respectively.

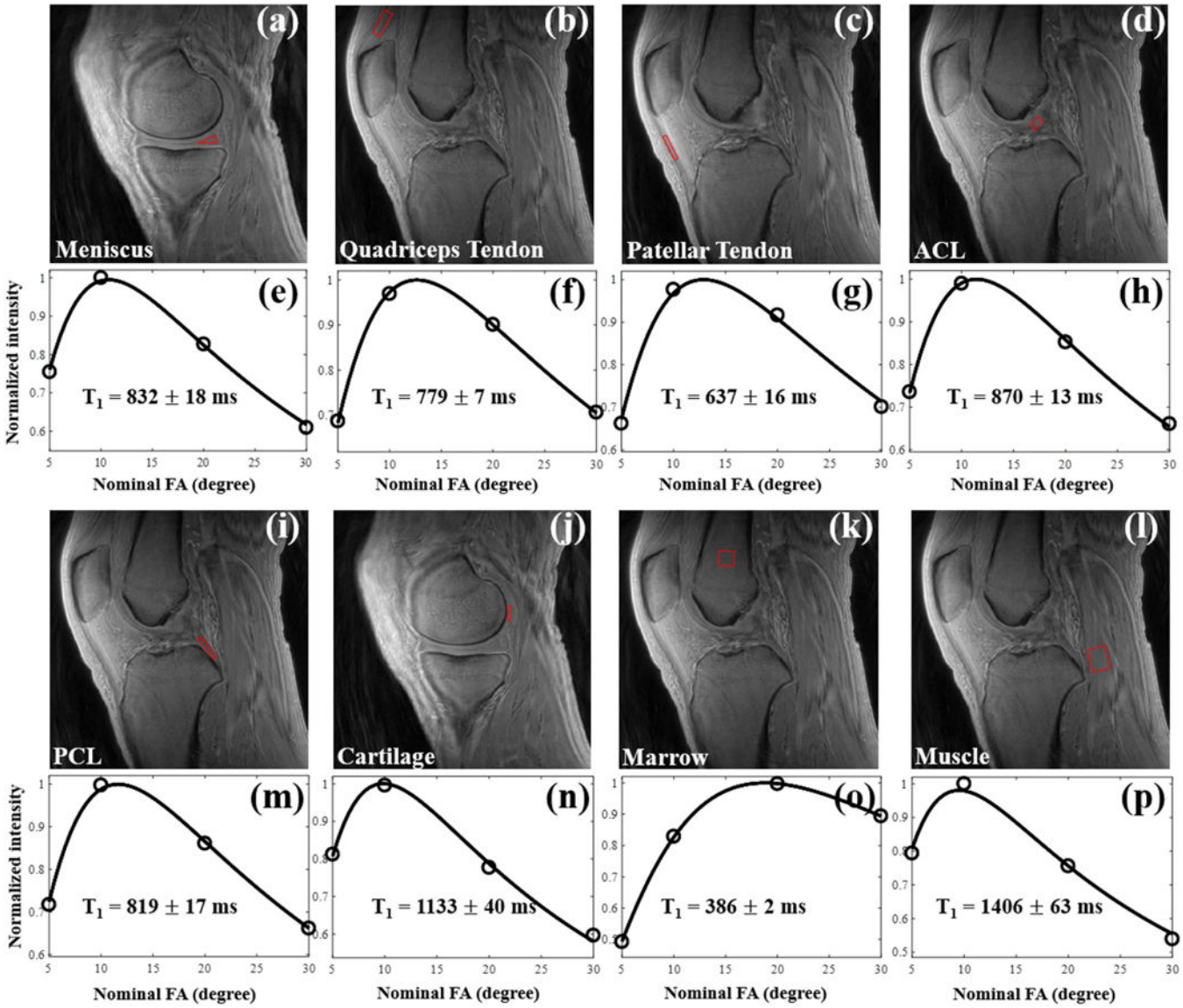

Figure 4.

T_1 fitting results in knee tissues from a representative healthy volunteer (age 35, male) using the proposed 3D UTE-Cones AFI-VFA method. The measured T_1 values for this volunteer were 832±18 ms for meniscus, 779±7 ms for quadriceps tendon, 637±16 ms for patellar tendon, 870±13 ms for ACL, 819±17 ms for PCL, 1133±40 ms for cartilage, 386±2 ms for marrow and 1406±63 ms for muscles.

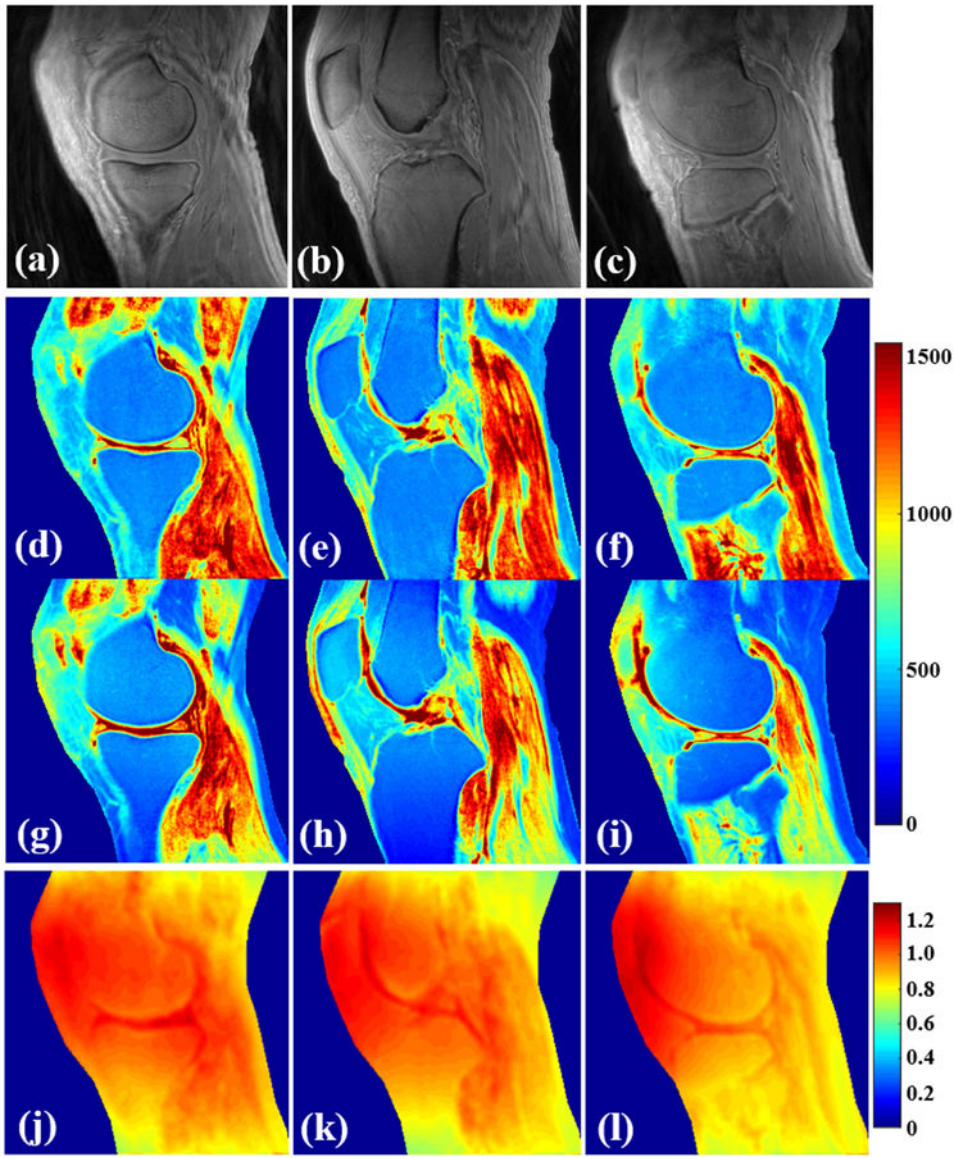

Figure 5.

Results in knee tissues from a healthy 35-year old male volunteer (a–l). (a–c) are the selected VFA images with FA = 5°. T_1 mapping using both the proposed 3D UTE-Cones AFI-VFA (d–f) and B_1-uncorrected VFA (g–i) methods are shown. The B_{1s} maps generated by the AFI technique (j–l) are shown. B_1 inhomogeneity induced T_1 estimation errors in the images of g–i have been corrected by the proposed 3D UTE-Cones AFI-VFA method, especially in regions close to the coil boundary.

Table 1

Mean and standard deviations of T_1 values of knee tissues of 16 healthy volunteers measured by the proposed 3D UTE-Cones AFI-VFA method.

Meniscus	Quadriceps tendon	Patellar tendon	ACL
833 ± 47 ms	800 ± 66 ms	656 ± 43 ms	873 ± 38 ms
PCL	**Cartilage**	**Marrow**	**Muscle**
832 ± 49 ms	1098 ± 67 ms	379 ± 18 ms	1393 ± 46 ms